Mem. S.A.It. Vol. 81, 757

Memorie della

On the energy flux in acoustic waves in the solar atmosphere

N. Bello González[1], M. Flores Soriano[2], F. Kneer[2], and O. Okunev[2,3]

[1] Kiepenheuer-Institut für Sonnenphysik, Schöneckstr. 6, D-79104 Freiburg, Germany
e-mail: nbello@kis.uni-freiburg.de
[2] Institut für Astrophysik, Friedrich-Hund-Platz 1, D-37077 Göttingen, Germany
[3] Central Astronomical Observatory of the Russian Academy of Sciences, Pulkovskoye chaussee 65/1, RU-196140 St. Petersburg, Russia

Abstract. The energy supply for the radiative losses of the quiet solar chromosphere is studied. Time sequences from quiet Sun disc centre were obtained with the "Göttingen" Fabry-Pérot spectrometer at the Vacuum Tower Telescope, Observatorio del Teide/Tenerife, in the non-magnetic Fe I 5576 Å line. The data were reconstructed with speckle methods. The velocities as measured at the line minimum were subjected to Fourier and wavelet analysis. The energy fluxes were corrected for the transmission of the solar atmosphere. We find an energy flux of $\sim 3\,000$ W m^{-2} at a height of $h = 250$ km. Approximately 2/3 of it is carried by waves in the 5–10 mHz range, and 1/3 in the 10–20 mHz band. The waves occur predominantly above inter-granular areas. We speculate that the acoustic flux in waves with periods shorter than the acoustic cutoff period ($U \approx 190$ s) can contribute to the basal heating of the solar chromosphere, in addition to atmospheric gravity waves.

Key words. Waves – Techniques: high angular resolution – Sun: chromosphere

1. Introduction

This contribution deals with the long lasting problem of energy supply to the solar chromosphere and stellar chromospheres. According to standard models of the quiet solar atmosphere, the net radiative losses from the chromosphere amount to $4\,600$ W m^{-2} (VAL C model, Vernazza et al. 1981). Including the radiative losses by the Fe II lines, Anderson & Athay (1989) arrive at a remarkable factor of 3 times more radiative losses, $14\,000$ W m^{-2}. Although the chromospheric radiation is 10^{-4} smaller than the output from the photosphere, it is the result of important physical processes. The chromosphere marks the transition from the photosphere in radiative equilibrium to the highly dynamic realms of outer atmospheric layers and the heliosphere.

Biermann (1948) and Schwarzschild (1948) suggested acoustic waves, generated by turbulent convection, for the energy transport and heating of the solar chromosphere. The theory of sound generation by turbulent flows was elaborated by Lighthill (1952) and Stein (1967). From the numerous subsequent studies we mention the work by Ulmschneider and his Heidelberg group (e.g., Fawzy et al. 2002), from which earlier work can be traced back. In these studies, numerical simulations were

Send offprint requests to: N. Bello González carried out to produce a chromospheric temperature rise as a result of shock dissipation of short-period waves , with periods in the range $U = 10 \ldots 100$ s.

It is extremely difficult to detect these the short-period waves observationally for two reasons. i) The contribution functions for the velocity/temperature information extend over a height range of at least 200 km which severely decreases any wave signal with periods shorter than ~ 60 s. ii) The waves are expected to have small horizontal extension.

The diverse results from observations and simulations of chromospheric heating by short-period waves are reviewed in Bello González et al. (2009b). Here we present results obtained from ground-based observations with high spatial resolution that concern the acoustic flux transported by short-period waves.

2. Observations and data analysis

The observations and the data analysis are described in detail in Bello González et al. (2009b). Here, a short delineation may suffice. The data were taken from quiet-Sun at disc centre on 2007 August 1. We used the Göttingen FPI spectrometer/polarimeter with its upgrades (Puschmann et al. 2006; Bello González & Kneer 2008) at the VTT/ Observatorio del Teide/Tenerife. The Fe I 5576 Å line was scanned with the spectrometer. A time sequence of ~ 22 min duration was analysed for the present study.

The broadband images were reconstructed with our speckle code (de Boer 1996). The reconstruction of the narrow-band images follows along the lines described repeatedly (e. g., Bello González et al. 2005).

The narrow-band images were subjected to a noise filter with a cutoff corresponding to $0\farcs3$.

The line profiles at each pixel and temporal position were smoothed with a wavelength filter. Then we determined the intensities and the Doppler shifts of the line minima from the parabola through the three intensities around the measured line minimum.

The images of the broadband time sequence were shifted to pixel accuracy to maximum correlation, and the identical shifts were applied to the Doppler shifts. A de-stretching of the broadband time sequence followed. The de-stretching parameters were then also applied to the velocity time series.

The further analysis and discussion was restricted to the central subfield of $23'' \times 23''$.

3. Response functions and atmospheric transmission

To determine the height of formation of the measured Doppler signals we calculated velocity response functions, $RF_v(z)$, with the method given by Eibe et al. (2001). The VAL C model atmosphere was used and the line profiles were calculated in LTE.

Figure 1 depicts the response functions. With infinite spectral resolution, the velocity signals at line minimum are formed at a height of approximately 400 km (dashed curve in Fig. 1). This agrees with the values given by Shchukina & Trujillo Bueno (2001). They obtained a height of 400 km in granules and 420 km in intergranules using non-LTE calculations of this line based on granular convection models for the optical depth $\tau_{\rm lc} = 1$.

However, when we apply the same spectrometric broadening and filtering in wavelength to the calculated line intensities as is for observed data, we obtain the solid curve in Fig. 1. Because of mixing of intensities around the line minimum, the response function has become broader and has moved down by approximately 150 km compared to the original one.

The broad contribution function severely reduces the measurable velocities of waves compared to the actual wave amplitudes. We calculated the transmission of wave *amplitudes* by imposing waves of small amplitude with periods U ranging from 30 s to 190 s onto the VAL C model (see details in Bello González et al. 2009b).

Figure 2 shows the resulting transmission function $T(U)$ for infinite spectral resolution and after applying the same convolution and wavelength filtering to the calculated line pro-

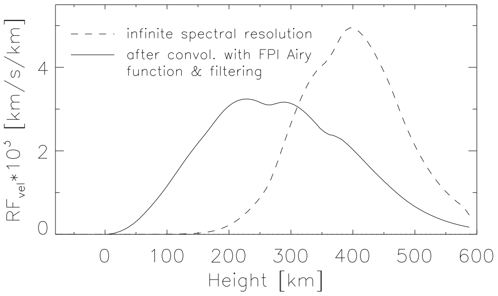

Fig. 1. Velocity response functions $RF_{\upsilon}(z)$ of the Fe I 5576 Å line in the VAL C model atmosphere and under LTE assumption.

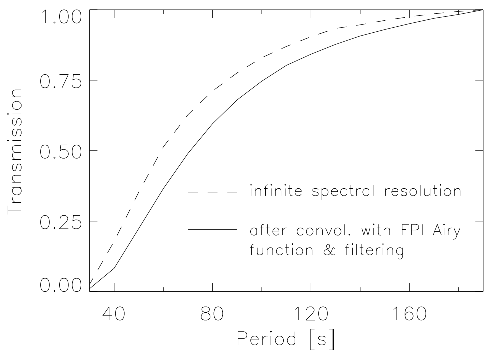

Fig. 2. Transmission function $T(U)$ of Fe I 5576 based on the VAL C atmosphere.

files as to the data. The square of the transmission is called *transfer function*.

4. Results

4.1. Fourier analysis

We calculated the temporal power spectrum of the line-minimum velocity at each pixel in the field-of-view (FOV). The dashed curve in Fig. 3 shows in its left panel the averaged power spectrum. The solid curve gives the power spectrum after applying a filter to the 3D data set which retains only waves in the acoustic domain of the k_{h}-ν diagram (k_{h} = horizontal wavenumber, e.g., Straus et al. 2008).

After subtraction of the noise level one may calculate estimates

$$F_{\mathrm{ac}}(\nu_i) = \rho P_{\upsilon}(\nu_i)\upsilon_{\mathrm{gr}}(\nu_i)/TF(\nu_i)\,, \qquad (1)$$

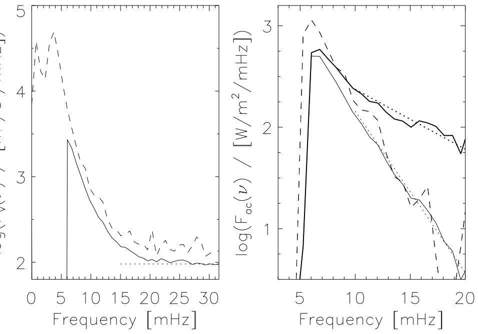

Fig. 3. Left panel: averaged temporal power spectra $P_{\upsilon}(\nu)$ of velocities; dashed: original data, solid: after high-pass filtering in k_{h} and ν; horizontal dotted line: noise level. Right panel: acoustic energy flux spectra $F_{\mathrm{ac}}(\nu)$ from the velocity power spectra; dashed: from original data, solid thin: after high-pass filtering, solid thick: high-pass filtered and corrected for transmission; dotted lines: slopes for extrapolation.

for the flux spectrum, with mass density ρ at the level of formation and group velocity υ_{gr}, and

$$F_{\mathrm{ac,tot}} = \sum_i F_{\mathrm{ac}}(\nu_i)\Delta\nu_i\,, \qquad (2)$$

for the total acoustic flux with summation over frequency intervals $\Delta\nu_i$. Dividing Eq. 1 by the *transfer function* $TF(\nu)$ includes the correction of the flux spectra. For the density we adopt the value $\rho = 5.4\times10^{-5}$ kg m^{-3} at a height of 250 km in the VAL C model. The right panel of Fig. 3 depicts the resulting acoustic flux spectra.

4.2. Wavelet analysis

We performed a wavelet analysis for the velocities in the acoustic domain. The code by Torrence & Compo (1988) was used with Morlet wavelets. We calculated the power in 20 s wide period bands between 50 s and 190 s. A statistical significance level of 95% was adopted. It could be demonstrated that the waves occur very intermittently (see Fig. 6 below and the movie with it, as well as Bello González et al. 2009b, Figs. 5 and 6).

The energy flux distribution $F_{\mathrm{ac}}(U)$ is given in Fig. 4. As for the the Fourier analy-

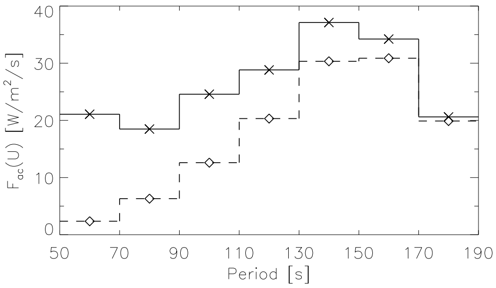

Fig. 4. Acoustic energy flux from wavelet analysis of the line-minimum velocities in the acoustic domain. Dashed and ◇◇◇: uncorrected for transmission; solid and × × ×: corrected.

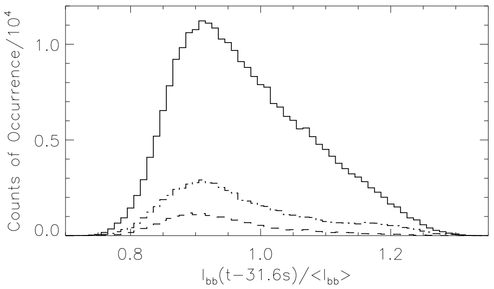

Fig. 5. Relation of wavelet power to broadband intensities in period bins 50–110 s (dashed), 110–150 s (dashed-dotted), and 150–190 s (solid). Only occurrences with power ≥ 0.3 of the maximum power in the specified period bins are included.

sis, the fluxes at shortest periods undergo the largest correction, by an average factor of 10 in the 50–70 s period bin.

The total acoustic flux is obtained, similarly as from Eqs. 1 and 2 above, by

$$F_{\mathrm{ac,tot}} = \Delta U \rho \sum_i < \upsilon_i^2 > \upsilon_{\mathrm{gr},i}/TF_i\,, \tag{3}$$

with summation over the period intervals.

Figure 5 demonstrates that the wave power is produced predominantly above the (dark) intergranular spaces. There the dependence of the occurrence of power in various period bands on the intensity of the broadband images is shown. For this comparison, the broadband images were taken two time steps (= 31.6 s) earlier than the occurrence of the wavelet power, which corresponds approximately to the travel time of the waves from $\tau_{\mathrm{cont}} = 1$ to the height of 250 km.

Animations of the granular evolution overlaid with power in various period bands confirm this finding Figure 6 shows a snapshot. Yet, one can also see power above small rapidly evolving granules, above granules before they split and above granular borders. Interestingly, the shorter the period and the smaller the power patches (typically ≤ 1), the more they occur in intergranules and in dark dots and lanes of granules. This is also visible in the slight shift of the curves in Fig. 5 towards smaller intensity values with decreasing periods.

Table 1 summarises the energy fluxes obtained from both Fourier and wavelet analysis.

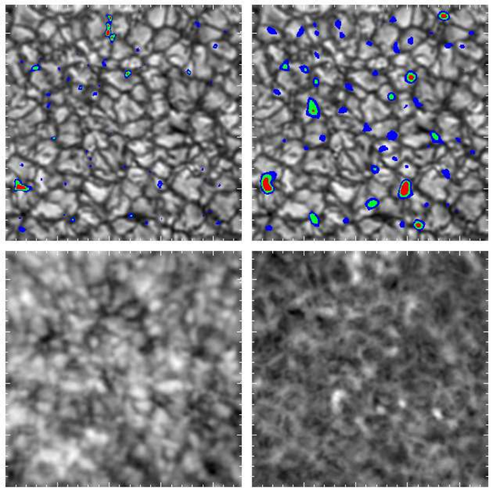

Fig. 6. Snapshot from a movie of granular evolution overlaid with occurrence of acoustic flux from velocity power Clockwise starting from upper left: granulation overlaid with wavelet power at periods 50–70 s, same but with periods 130–150 s, velocity and line-minimum intensity. Contours represent acoustic flux of 2 000, 3 000 and 4 000 W m^{-2}.

We find, after correction for atmospheric transmission, a total flux of 2 500–3 500 W m^{-2} at 250 km height. Approximately 2/3 of the flux is carried by waves with frequencies of 5.2–10 mHz and 1/3 of it by waves with frequencies of 10–20 mHz. We also measured separately the acoustic energy flux in regions of persistently low and high line-minimum intensities, used as proxies for small and large magnetic

Table 1. Energy flux of acoustic waves at 250 km; (un-)corrected: (no) correction for transmission; *lower limits*: correction for transmission with infinite spectral resolution.

	F_{ac} [W m^{-2}]		
	5.2–10 mHz	10–20 mHz	total
Fourier			
uncorrected	1 500	340	1 840
corrected	1 910	1 280	3 190
lower limits	*1 720*	*780*	*2 500*
wavelets			
uncorrected	2 150	310	2 460
corrected	2 630	1 020	3 650
lower limits	*2 410*	*630*	*3 040*

flux, respectively. A difference in the acoustic flux was not seen.

We extrapolate the acoustic flux distributions to frequencies higher than 20 mHz according to the slopes in Fig. 3 and integrate over period. The additional flux, corrected for atmospheric transmission, amounts to 450 W m^{-2}. An extrapolation of the corrected flux distribution from the wavelet analysis to a lower limit of short-period waves with $U = 10$ s yields an additional flux of 840 W m^{-2}.

As an outlook, we show in Fig. 7 preliminary results from observations in Fe I 5434. The velocity signal of the minimum of this line, i.e., where $\tau_{lc} \approx 1$, is said to be formed around the temperature minimum in standard atmospheric models. The total acoustic flux found here, after correction for atmospheric transmission, is estimated to 1 900 W m^{-2}. Extrapolation of the flux distribution yields an additional flux of ~ 400 W m^{-2}.

5. Discussion and conclusions

From two different methods, a Fourier and wavelet analysis, respectively, we obtained approximately the same estimate of 2 500–3 500 W m^{-2} for the acoustic flux at 250 km. Preliminary results from Fe I 5434 Å data give 1 900 W m^{-2}. A decrease with height

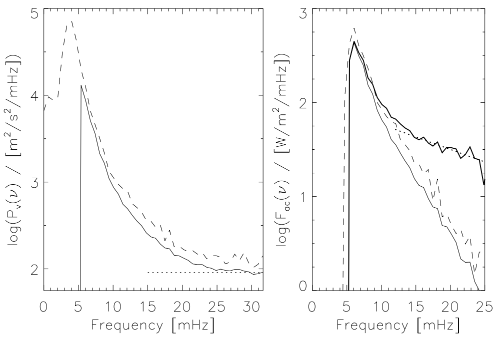

Fig. 7. Preliminary result for power and flux spectra measured in Fe I 5434, data from 2009 May 12.

caused by radiative damping is expected (e.g., Straus et al. 2008). The measured fluxes are too low by a factor of ~ 2 to account for the chromospheric radiative losses, as required by the VAL C model of the mean chromosphere. Are they sufficient for a basal flux (Schrijver 1987) from very quiet, non-magnetic areas?

Yet the fluxes found here are 3–6 times larger than those found by Fossum & Carlsson (2006) from TRACE continuum data and by Carlsson et al. (2007) from HINODE Ca II H filtergrams. These measurements suffer from either too low spatial resolution or from contribution functions which are very extended in height. It appears that it is much more reliable to determine mechanical fluxes from Doppler shifts, which measure gas motions, than from intensity fluctuations formed in non-LTE.

Straus et al. (2008) obtained an acoustic flux of 1 400 W m^{-2} also at 250 km. This is 30% lower than our uncorrected value of 1 840 W m^{-2}, probably because our data analysis with speckle reconstruction gives somewhat higher spatial resolution. Straus et al. (2008) also found a substantial flux in atmospheric gravity waves of 5 000 W m^{-2} at 500 km. Such measurements are extremely difficult for two reasons. i) One needs to determine the height of formation of velocities in at least two different spectral features/line depressions. Our experience shows that the response functions for bisector shifts are too extended in height (cf. Fig. 1). ii) The signature of the granular motion has to be eliminated carefully, especially for short-lived granules.

In view of the inhomogeneous atmospheric structure and dynamics, the determination of formation height assuming a homogeneous, static atmospheric model in LTE is problematic, to say the least. Likewise, the application of correction functions for the reduction of the transmission by the atmosphere itself and by the measurement process is far from being accurate. The corrections for the velocity power amount to one order of magnitude at 20 mHz. Yet we know that the reduced transmission plays an important role for the flux determination.

Especially the highly spatial and temporal intermittency of the waves, as revealed by our wavelet analysis, demonstrates the generation and propagation of waves in strong inhomogeneities. In view of this, an analysis in the Fourier domain, i.e., in the $k_{\mathrm{h}} - \nu$ plane looses its meaning. A small-scale excitation in form of a kind of explosion leaves its signature everywhere in this plane.

We consider it an important next step to guide the interpretation of velocity/intensity fluctuations in the solar atmosphere by numerical simulations as in Wedemeyer-Böhm et al. (2007), Straus et al. (2008), and recently for magnetic field dynamics in Bello González et al. (2009a). One-dimensional calculations with wave spectra in a model atmosphere do not appear sufficient as pointed out by Ulmschneider et al. (2005). They are misleading because shock merging destroys much of the short-period power.

3D simulations become feasible with today's computer facilities and with the codes being developed. Simulations with high temporal and spatial resolution are definitely needed. They should include the production of acoustic waves by the granular convection and their propagation through the inhomogeneous solar photosphere. They will take the lead in the interpretation of what is seen in high resolution observations.

Acknowledgements. NBG acknowledges financial support by the Kiepenheuer-Institut für Sonnenphysik through the *Pakt für Forschung und Innovation* of the WGL. MFS held a grant from the ERASMUS program of the European Union. OO thanks for support by Deutsche Forschungsgemeinschaft through grant KN 152/29-3 and by the Institut für Astrophysik Göttingen. Wavelet software was provided by C. Torrence and G. Compo, and is available at URL: http://paos.colorado.edu/research/wavelets.

References

Anderson, L. S., & Athay, R. G. 1989, ApJ, 346, 1010
Bello González, N., & Kneer, F. 2008, A&A, 480, 265
Bello González, N., et al. 2005, A&A, 434, 317
Bello González, N., et al. 2009, A&A, 494, 1091
Bello González, N.,et al. 2009, A&A, 508, 941
Biermann, L. 1948, ZAp, 25, 161
Carlsson, M., et al. 2007, PASJ, 59, 663
de Boer, C. R. 1996, A&AS, 120, 195
Eibe, M. T., et al. 2001, A&A, 371, 1128
Fawzy, D., et al. 2002, A&A, 386, 971
Fossum, A., & Carlsson, M. 2006, ApJ, 646, 579
Lighthill, M. J. 1952, Proc. R. Soc. London, 211, 564
Puschmann, K. G., et al. 2006, A&A, 445, 337
Schrijver, C. J. 1987, A&A, 172, 111
Schwarzschild, M. 1948, ApJ, 107, 1
Shchukina, N., & Trujillo Bueno, J. 2001, ApJ, 550, 970
Stein, R. F. 1967, Sol. Phys., 2, 385
Straus, T., et al. 2008, ApJ, 681, L125
Torrence, C., & Compo, G. P. 1998, Bull. Amer. Meteor. Soc., 79, 61
Ulmschneider, P., et al. 2005, ApJ, 631, L155
Vernazza, J. E., Avrett, E. H., & Loeser, R. 1981, ApJS, 45, 635
Wedemeyer-Böhm, S. et al. 2007, in The Physics of Chromospheric Plasmas, ed. I. Dorotovič, P. Heinzel, & R. J. Rutten, ASPCS, 368, 93